



Supplement of

Two decades observing smoke above clouds in the south-eastern Atlantic Ocean: Deep Blue algorithm updates and validation with ORACLES field campaign data

Andrew M. Sayer et al.

Correspondence to: Andrew M. Sayer (andrew.sayer@nasa.gov)

The copyright of individual parts of the supplement might differ from the CC BY 4.0 License.

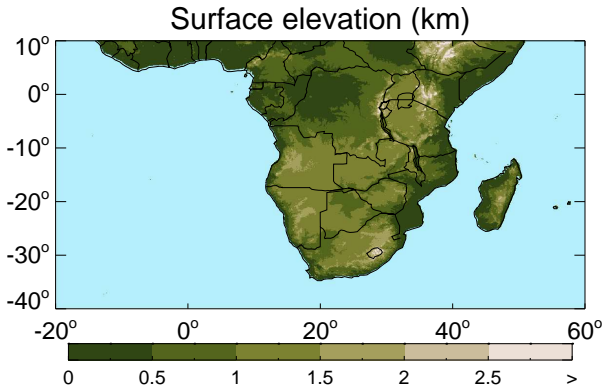


Figure S1. Surface elevation over the study region from the GTOPO30 digital elevation model. Regions at or below sea level are coloured pale blue.

This Supplement contains several Figures relating to the AAC algorithm's treatment of surface pressure and reflectance. They are referenced in the main text of the paper.

1 Surface elevation

Figure S1 shows surface elevation over the study region from the Gridded Topography at 30 arc second resolution (GTOPO30) 5 digital elevation model (Gesch and Larson, 1996; Gesch et al., 1999).

2 Land surface reflectance

As described in the paper's main text, the source MCD43GF data (Sun et al., 2017) are spatiotemporally aggregated to provide a data base for a representative year (retaining the 8-day time steps) at 0.05° resolution. As a measure of the uncertainty introduced by this spatial coarsening, Figure S2 shows the mean of the spatial standard deviation of albedo within each grid cell.

10 After the spatial aggregation, for each grid cell, spectral band, and eight-day period (out of 46 in a year), the median albedo from up to 13 years is taken as representative of that location and time of year. This collapses the interannual variation to provide, for each point, the annual cycle of surface albedo, which is used in the AAC retrieval. Figure S3 shows the mean (across all eight-day periods) temporal standard deviation (across the 13 years) of surface albedo, i.e. a measure of the interannual variability at each location.

15 The resulting annual cycles of surface albedo are shown for four sample locations, representing different surface types, in Figure S4. The Namibian sand dunes and rainforest in Congo show very little variability throughout the year, indicating little change in surface cover. In contrast the farmland shows an annual cycle, related to the phenological cycle of plant growth and resulting agricultural patterns. The semi-arid example (from the Kalahari Desert in Botswana) shows less seasonal variability, but more interannual variability.

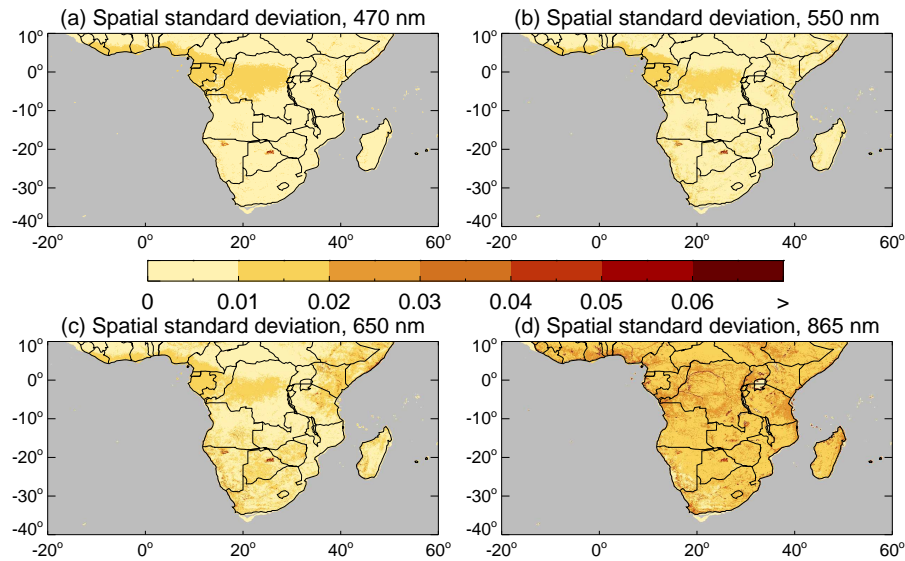


Figure S2. Mean spatial variability in MCD43GF surface albedo within each 0.05° grid cell, for all available data within the period 2003–2015. Grid cells in grey denote areas without MCD43GF coverage.

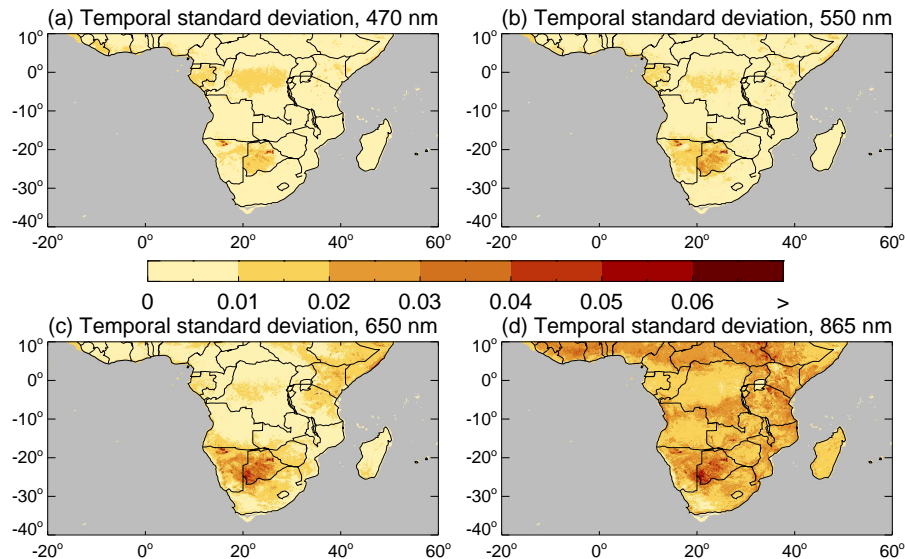


Figure S3. As Figure S2, except for the mean interannual variability in MCD43GF surface albedo within a given 8-day period over the year.

References

- Gesch, D. B. and Larson, K. S.: Techniques for development of global 1-kilometer digital elevation models, in: Pecora Thirteen Human Interactions with the Environment-Perspectives from Space, 1996.

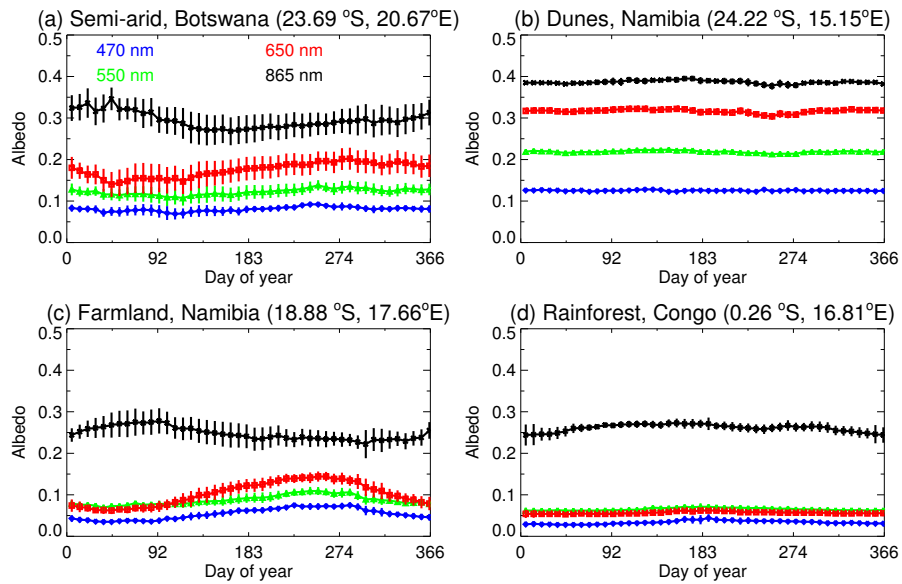


Figure S4. Climatological annual cycle of surface albedo for four different land cover types across the study region. Data shown for 470 nm (blue), 550 nm (green), 650 nm (red), and 865 nm (black) bands. Points show multiannual median values, and vertical bars the interannual standard deviation.

Gesch, D. B., Verdin, K. L., and Greenlee, S. K.: New land surface digital elevation model covers the earth, *Eos, Transactions, American Geophysical Union*, 80, 69–70, <https://doi.org/10.1029/99EO00050>, 1999.

5 Sun, Q., Wang, Z., Li, Z., Erb, A., and Schaaf, C. B.: Evaluation of the global MODIS 30 arc-second spatially and temporally complete snow-free land surface albedo and reflectance anisotropy dataset, *International Journal of Applied Earth Observation and Geoinformation*, 58, 36–49, <https://doi.org/10.1016/j.jag.2017.01.011>, 2017.